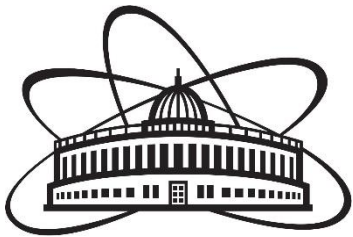
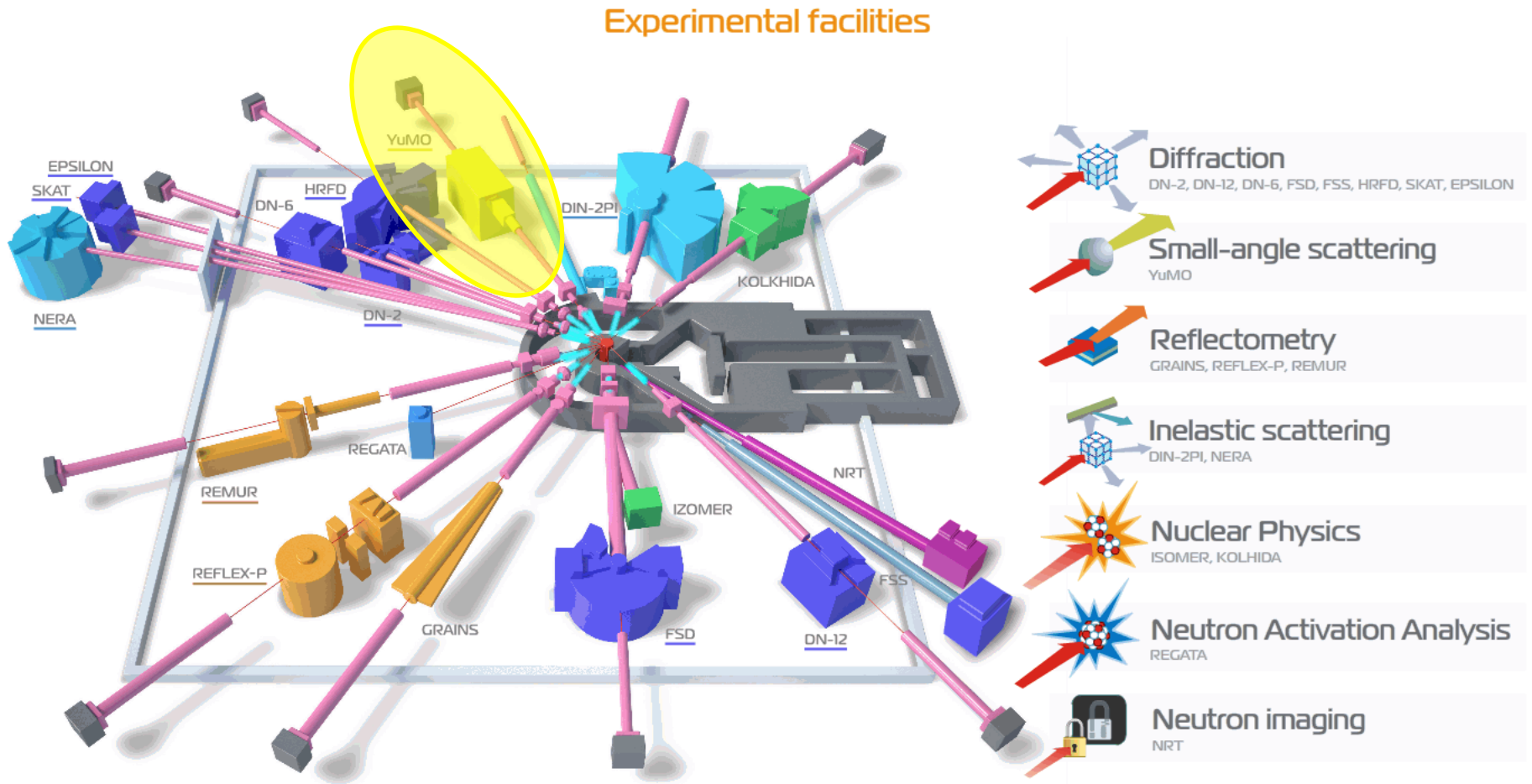


# *Small Angle Neutron Scattering at the IBR-2 and Science*

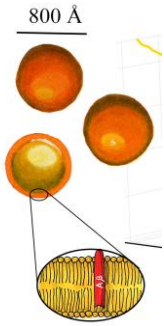
*O.I. Ivankov, T.N. Murugova, A.Kh. Islamov, A. Nabiev,  
S.A. Kurakin, A.V. Rogachev, V.V. Skoi, A.H.A. Elmekawi,  
M. Balasoiu, Yu.S. Kovalev, Yu.L. Rzykaiu, A.V. Vlasov,  
A.G. Soloviev, V. Gordeliy, N. Kucerka, and A. I. Kuklin*



# Suite of Spectrometers



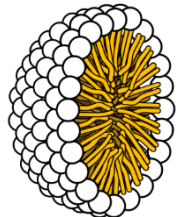
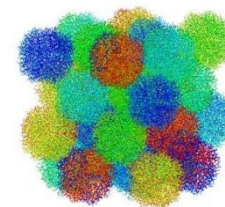
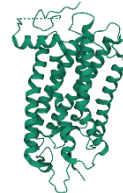
# Small Angle Scattering



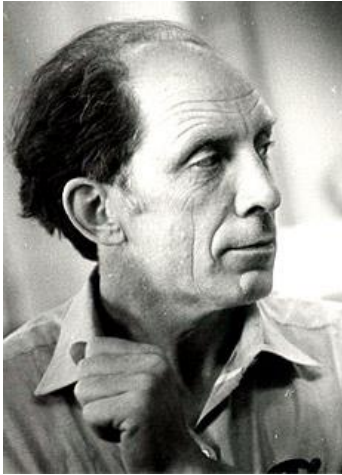
Structural information:  
10-1000 Å

- Biology
  - Colloidal chemistry
  - Material science
  - Solid state physics
  - Polymers physics
- 
- Macromolecules and its aggregates in solvents
  - Alloys
  - Films
  - Powders

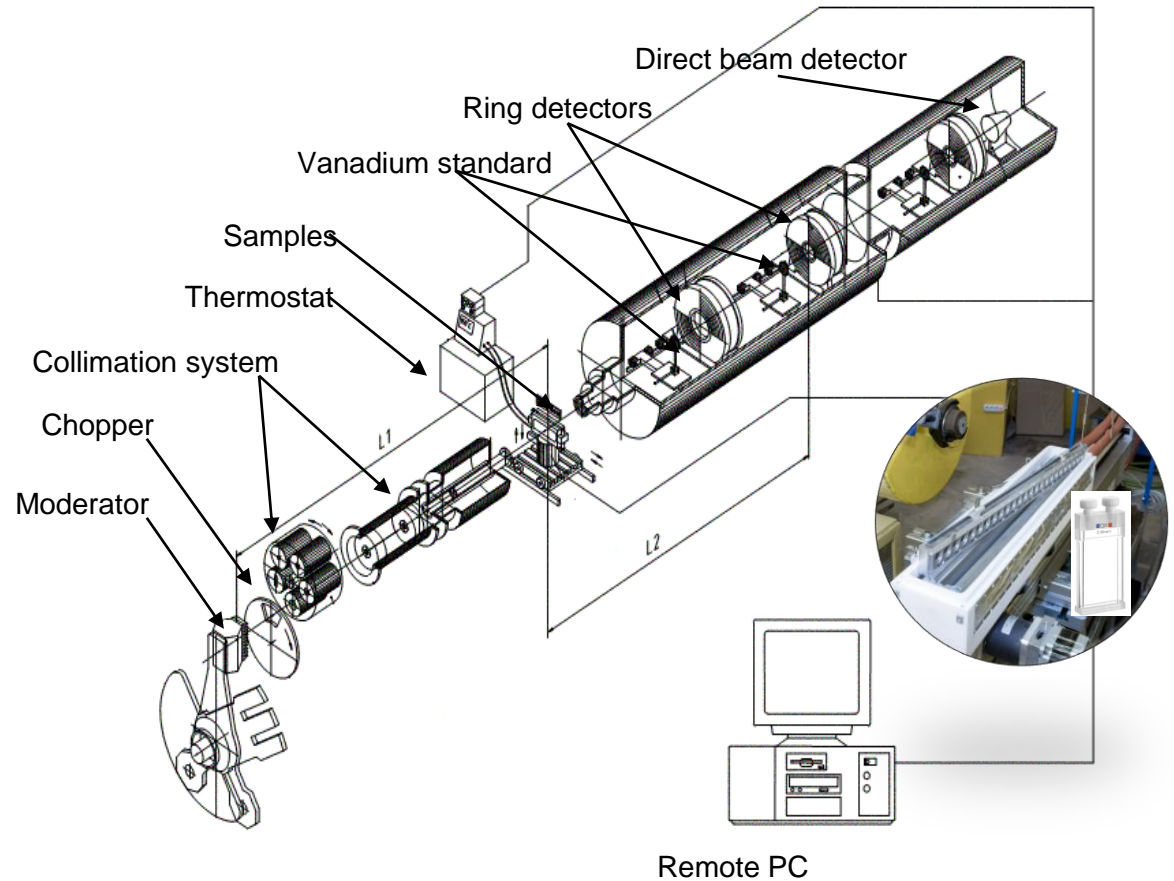
- Size, volume, molecular weight
- Shape
- Conformation
- Oligomeric state
- 3D structures with resolution  $\sim 10$  Å



# YuMO Spectrometer



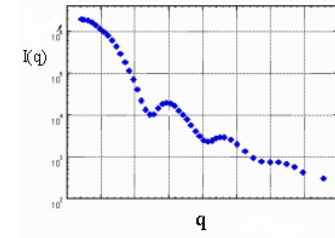
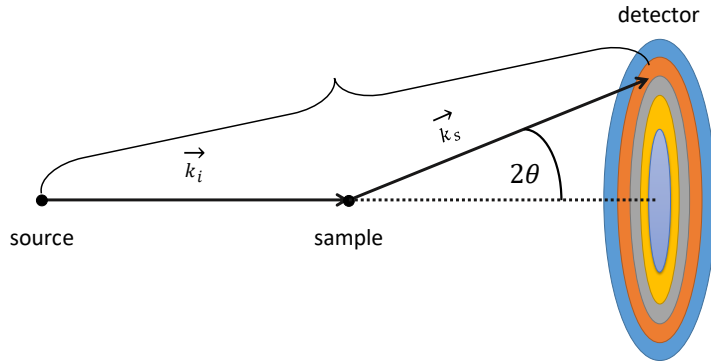
Yuri  
Mechislavovich  
Ostonevich



В.А.Вагов, А.Б.Кунченко, Ю.М.Останеvич, И.М.Саламатин, Установка малоуглового рассеяния нейтронов по методу времени пролета на импульсном реакторе ИБР-2// Сообщения ОИЯИ, Р14-83-898, Дубна, 1983.

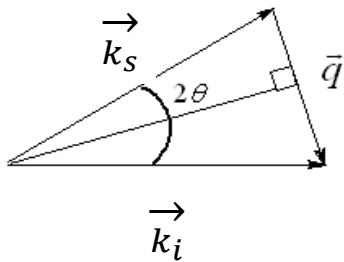
Kuklin, A.I., Ivankov O.I., Rogachev A.V., Soloviev D., Islamov A., Skoi V.V., Kovalev Y., Vlasov A., Rizhikau Y.L., Soloviev A., Kucerka N., Gordeliy V., *Small-Angle Neutron Scattering at the Pulsed Reactor IBR-2: Current Status and Prospects*. Crystallography Reports, 2021. **66**(2): p. 230-241.

# SANS experiment scheme



Scattering curve

$$I(q) = \frac{d\sigma}{d\Omega} = \iint_V \rho(\vec{r}_i) \rho(\vec{r}_k) \frac{\sin q|\vec{r}_i - \vec{r}_k|}{q|\vec{r}_i - \vec{r}_k|} d\vec{r}_i d\vec{r}_k.$$



$$\vec{q} = \vec{k}_i - \vec{k}_s$$

Scattering vector  $q$

$$\lambda = \text{const}$$

or

$$q = 2k \sin \theta = \frac{4\pi}{\lambda} \sin \theta$$

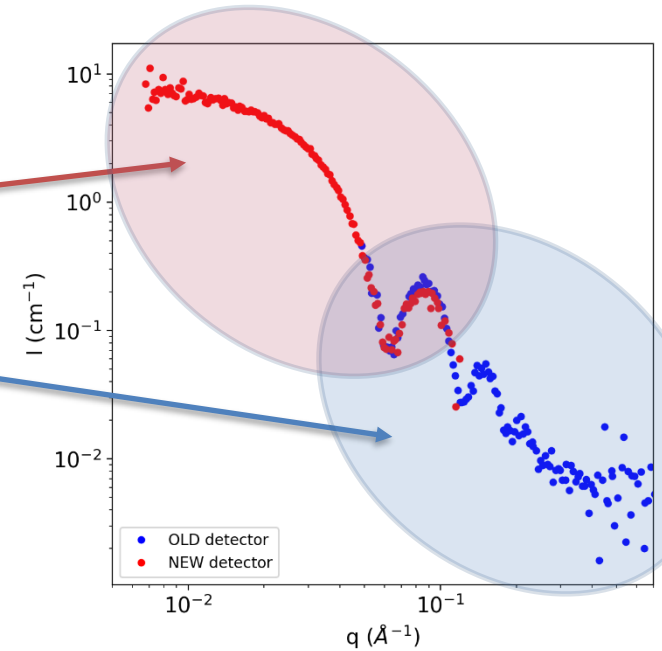
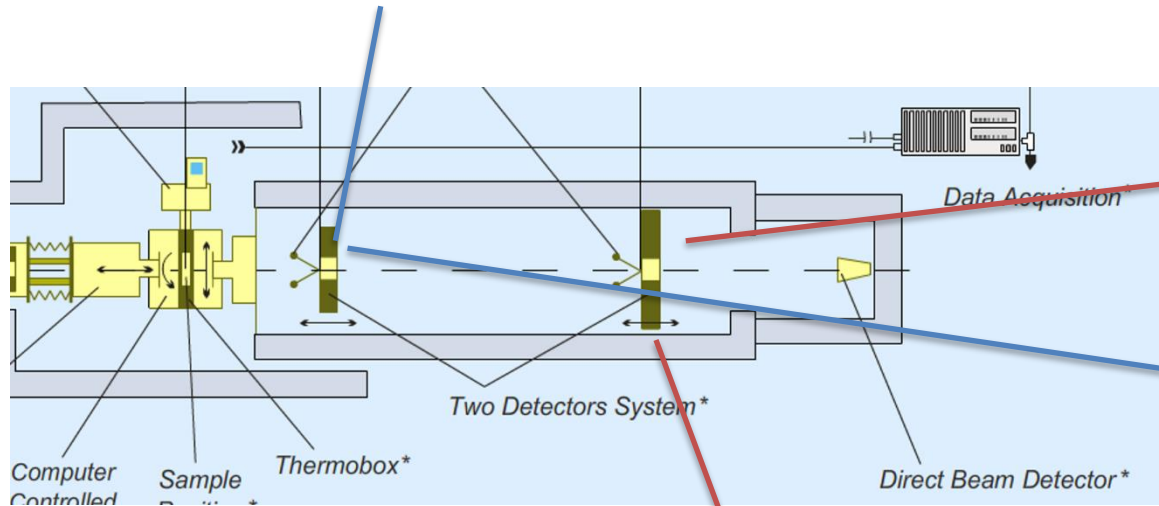
$$\lambda = \frac{h}{mv} = \frac{t \cdot h}{m \cdot L}$$

# Two-detector system of YuMO



1978 y.

Б.Н.Ананьев, А.Б.Кунченко, В.И.Лазин, Ю.М.Останевич,  
Е.Я.Пикельнер, Кольцевой многонитевой детектор медленных  
нейтронов с гелием-3 // Сообщения ОИЯИ, 3-11502, Дубна, 1978.



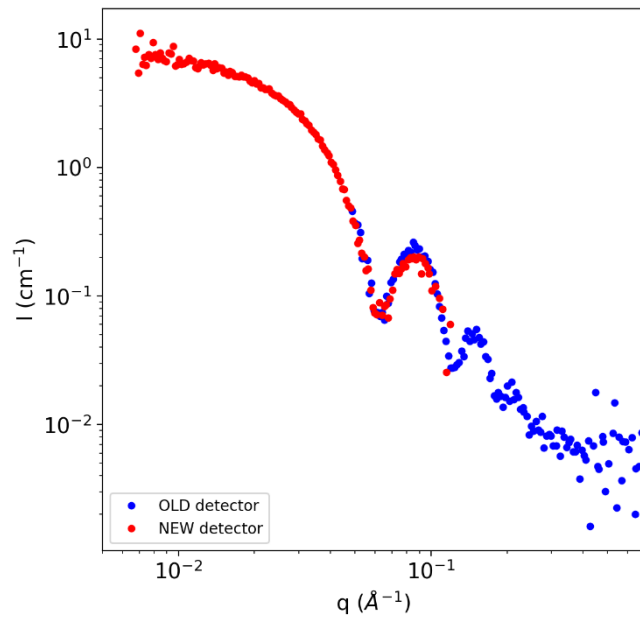
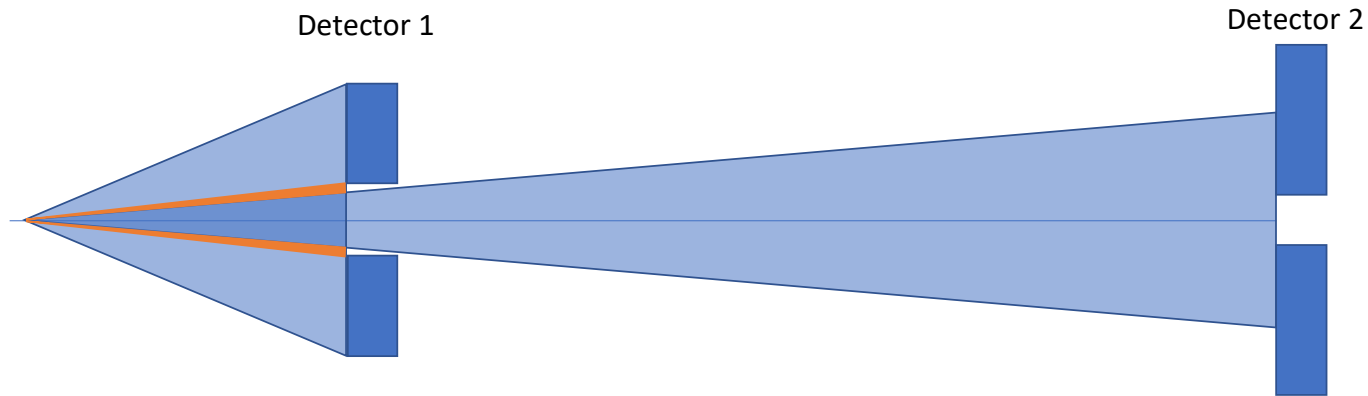
1983 y.



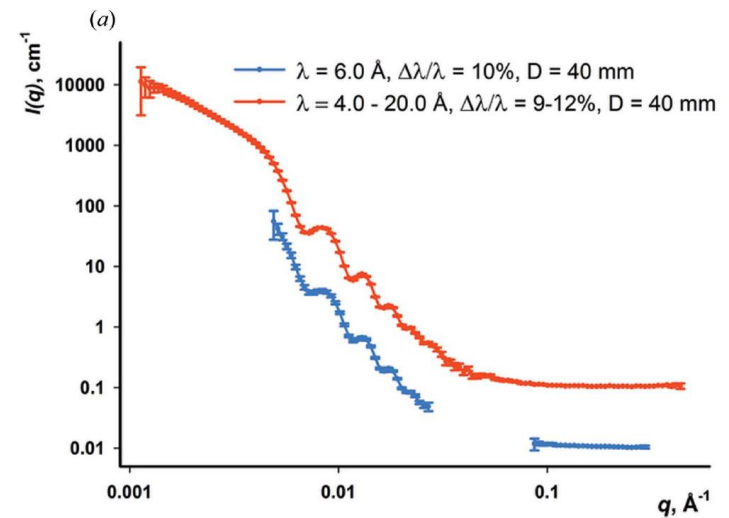
$$\frac{q_{max}}{q_{min}} = 100$$

\* For the thermal neutrons spectra<sub>6</sub>

# Two-detector system of YuMO



YuMO spectrometer



Spectrometer BILBY (ANSTO, Australia)

Anna Sokolova et al., Performance and characteristics of the **BILBY** time-of-flight small-angle neutron scattering instrument // *J. Appl. Cryst.* (2019). **52**, 1-12

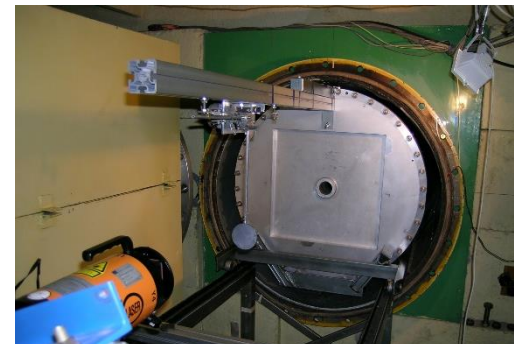
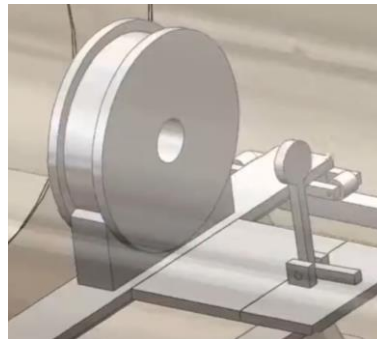
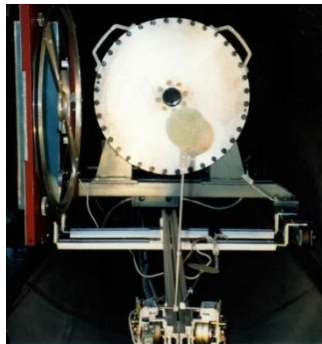
# Raw spectra data treatment

$$I(\theta, \lambda) = I_0(\lambda) \cdot \frac{d\Sigma}{d\Omega} \cdot \epsilon(\lambda) \cdot e^{-\Sigma_t(\lambda)d_s} \cdot \Omega_s + B(\theta, \lambda)$$

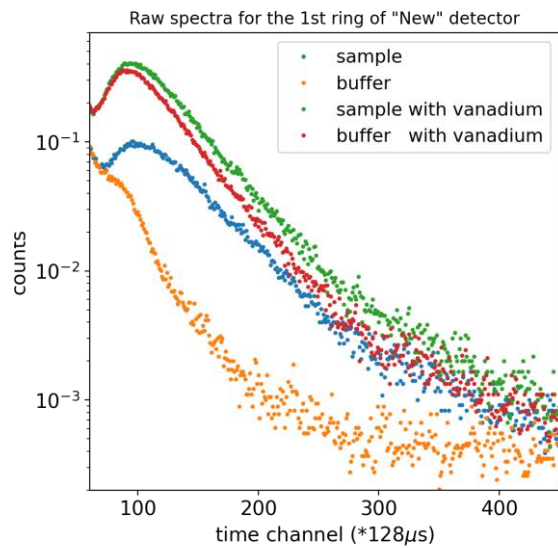
Incident beam
Detector effectivity
Sample transmission
Solid angle
Background

Differential cross section

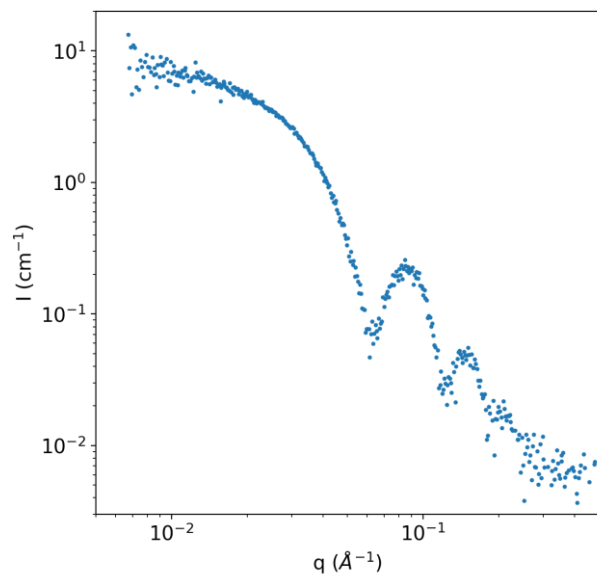
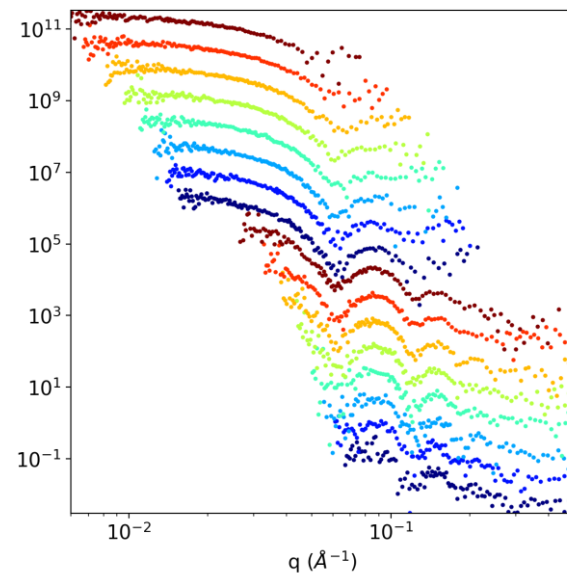
$$\frac{d\Sigma}{d\Omega} = \frac{I_{sample} - I_{buffer}}{I_{sv} - I_{sample}} \cdot \frac{\Omega_v}{\Omega_s} \cdot T_v \cdot d_v \cdot \left(\frac{d\Sigma}{d\Omega}\right)_v \cdot \frac{1}{d_s}$$



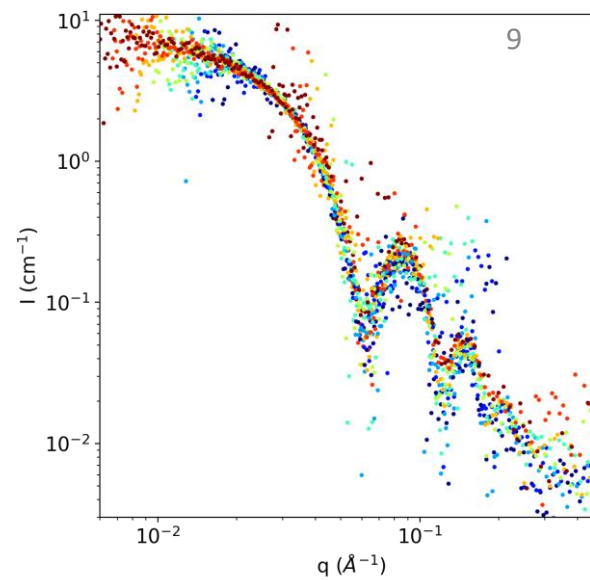




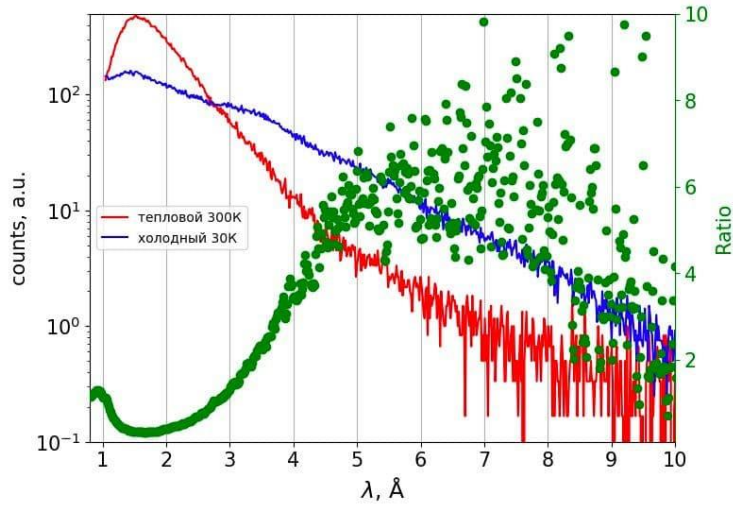
$$\frac{d\Sigma}{d\Omega} = \frac{I_{sample} - I_{buffer}}{I_{sv} - I_{sample}} \cdot \frac{\Omega_v}{\Omega_s} \cdot T_v \cdot d_v \cdot \left(\frac{d\Sigma}{d\Omega}\right)_v \cdot \frac{1}{d_s}$$



Averaging



# Cold moderator



gain factor wavelength

(1Å-3Å): 0.47

(1Å-6Å): 0.65

(1Å-8Å): 0.67

(1Å-10Å): 0.67

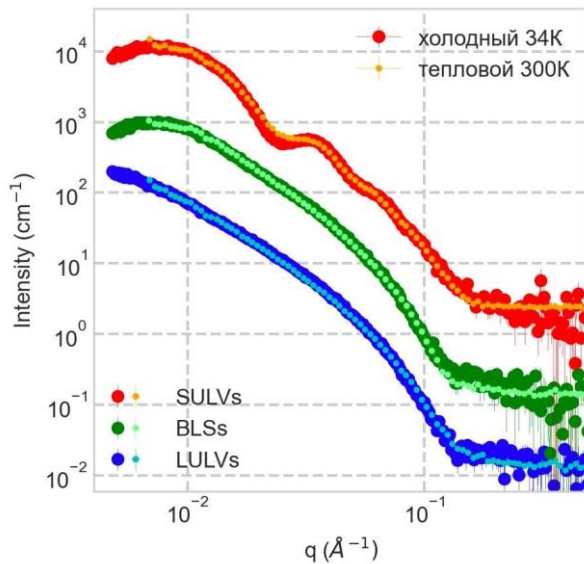
(3Å-10Å): 3.02

Gain Factor (Ratio):

min ~ 0.3 (1.5 Å)

max ~ 6 (> 5Å)

Comparison of the counts on the detectors with the cold moderator at ~ 300K and ~34K



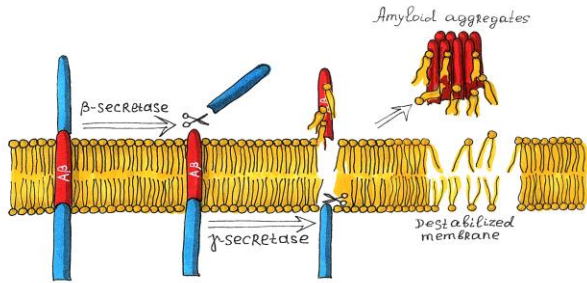
Dynamic q-range

$$\frac{q_{max}}{q_{min}} = 140$$

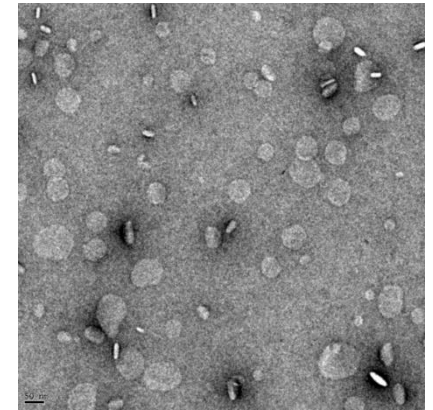
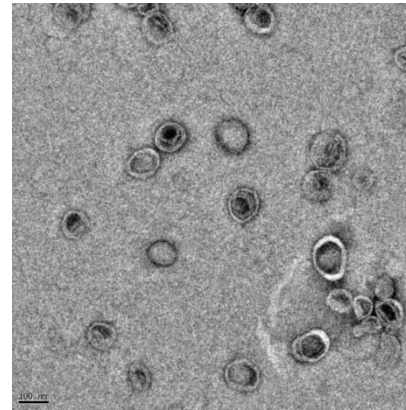
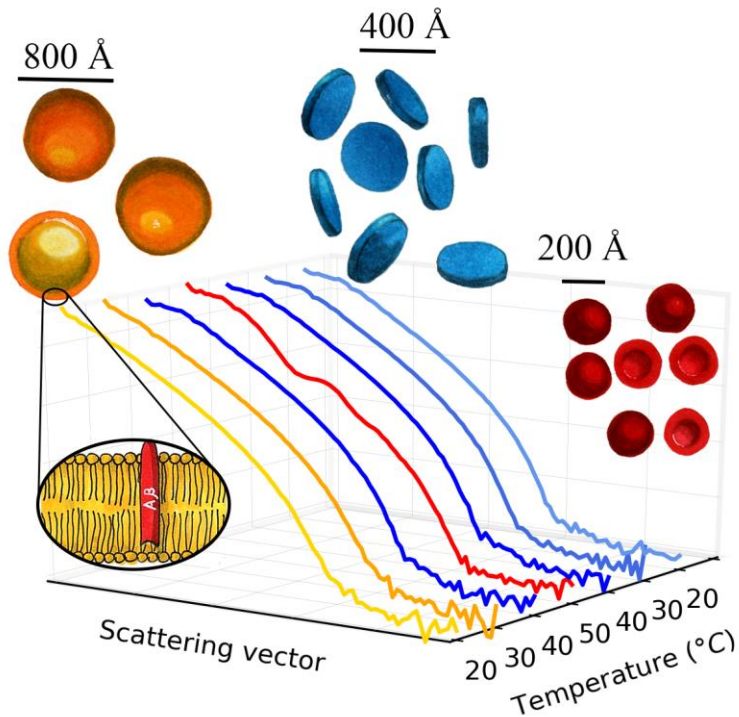
## Parameters of YuMO spectrometer

<b>Flux on the sample</b> (thermal neutrons)	$10^7 - 4 \times 10^7 \text{ n}/(\text{s cm}^2)$
<b>Used wavelength</b>	0.5 Å to 8 Å (10Å with cold moderator 30K)
<b>Q-range</b>	0.007 – 0.7 Å <sup>-1</sup> (0.005-0.7 Å <sup>-1</sup> cold moderator)
<b>Dynamic Q-range</b>	$q_{\text{max}}/q_{\text{min}}$ up to 100 (140 cold moderator)
<b>Specific features</b>	Two detectors system, central hole detectors
<b>Size range of the structural features under investigation</b>	1000 – 10 Å
<b>Intensity</b> (absolute units -minimal levels)	0.01 cm <sup>-1</sup>
<b>Calibration standard</b>	Vanadium during the experiment
<b>Beam dimension at the sample position</b>	14 mm diameter
<b>Collimation system</b>	Axial
<b>Detectors</b>	He <sup>3</sup> -filed, in-house design, 8 independent wires
<b>Detector</b> (direct beam)	<sup>6</sup> Li-converter (in-house design)
<b>Sample changer</b>	In-house designed box, in air
<b>Q-resolution</b>	5-15%
<b>Temperature range</b>	4°C - + 70°C (standard Hellma cells, 1mm, 2 mm) -20°C - + 130°C (in-house design sample holders)
<b>Number of the samples in the automated sample changer</b>	25
<b>Average single data collection time</b>	1 h
<b>Reactor pulse frequency</b>	5 Hz

# Interactions in Disease Modeling Membranes



Neutron scattering allows to study model membranes that replicate pre-clinical conditions of **Alzheimer's disease**



TEM images of the DMPC (left) and DMPC/A $\beta$ 25-35 (right) systems collected at 20°C. The dark bars (100 and 50 nm, respectively) in the lower left corners allow to assess the length scales. Objects in the left-hand panel match the typical vesicular objects with mostly unilamellar walls. The right-hand panel reveals randomly oriented discs also consisting of single layers.

Changes in the membrane self-organization happen during the thermodynamic phase transitions of lipids and are interpreted as the **peptide driven membrane damage**.

Ivankov O., Murugova T.N., ..., Kučerka N., *Scientific Reports* (2021).

# Kinetics system for YuMO spectrometer

Time of measurement – 2 min

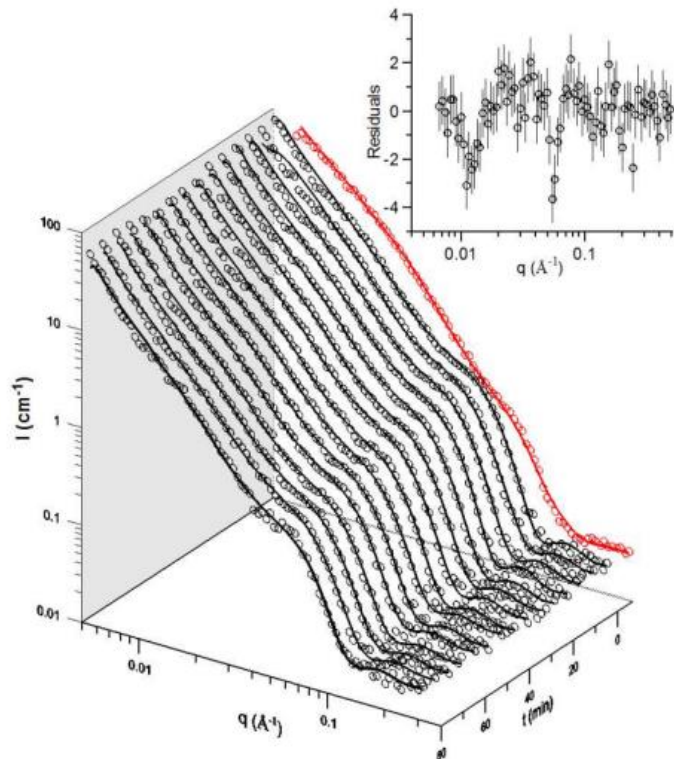


Figure 4. Dependences of SANS intensity  $I(q)$  on scattering vector  $q$  for DNA –  $\text{C}_{12}\text{NO}/\text{DOPE}$  dispersion as a function of time; prior (red points) and after DCI injection. Full lines show fits using a paracrystal lamellar model.

Inset: An example of the distribution of residuals.

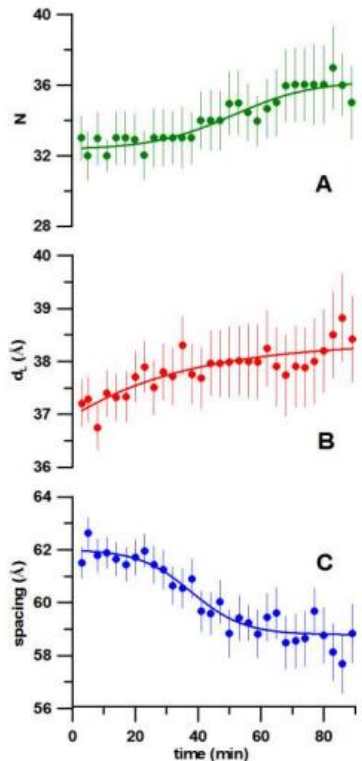
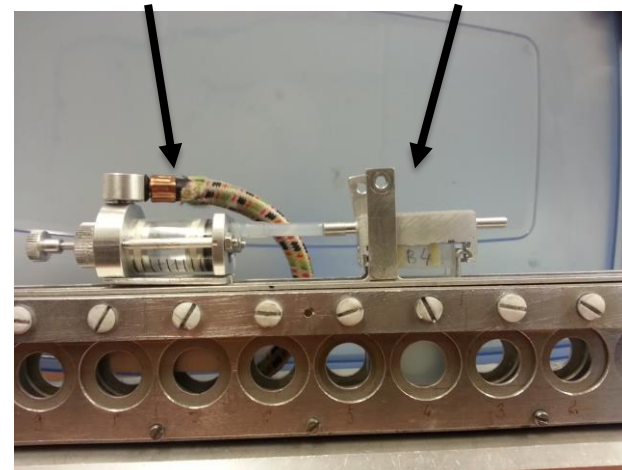


Figure 5. Time dependence of the structural parameters: the number of layers (A), the lipid bilayer thickness (B) and the spacing (C).

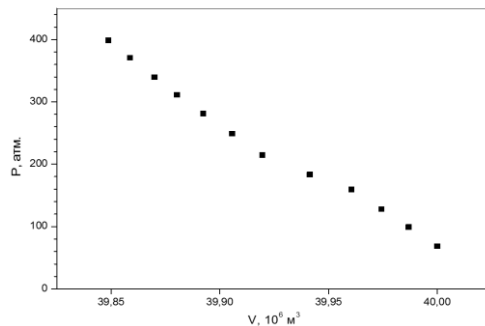
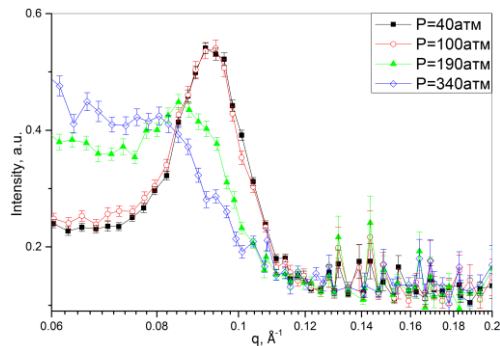
Container for the sample to be injected

Standard cuvette

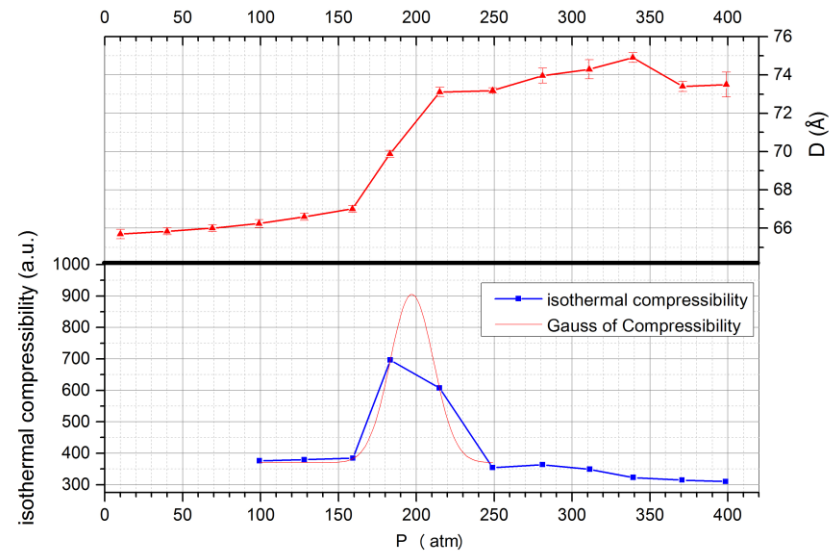
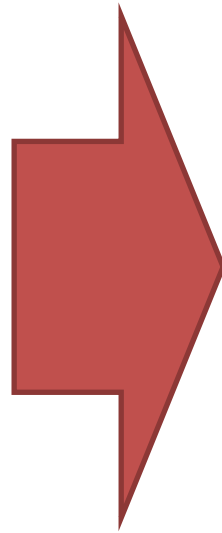


Sample holder

# Volumetric setup for YuMO spectrometer



- Volume of the sample required: 3-4 ml
- Pressure up to 2 kBar



# Size-exclusion chromatography (SEC)

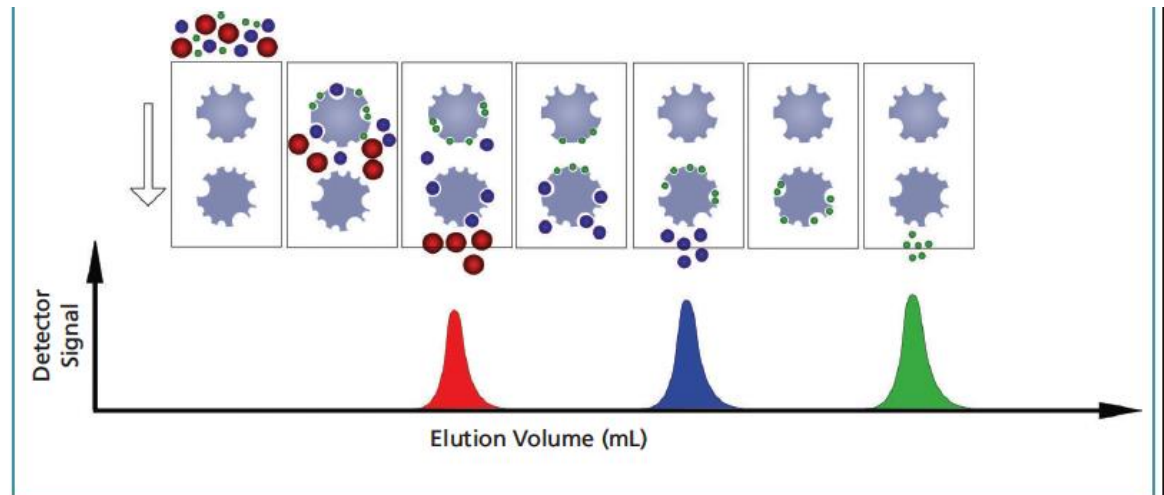


## Applications:

- Separation of macromolecules from complex mixtures according to their size, charge, selective non-covalent interaction and other properties.
- Protein and polymers purification.
- Affinity-tagged protein purification.
- Desalting and buffer exchange.
- Identification and quantitation of macromolecules (evaluation of hydrodynamic size of a macromolecule).
- Detects the unknown compounds and purity of mixture.

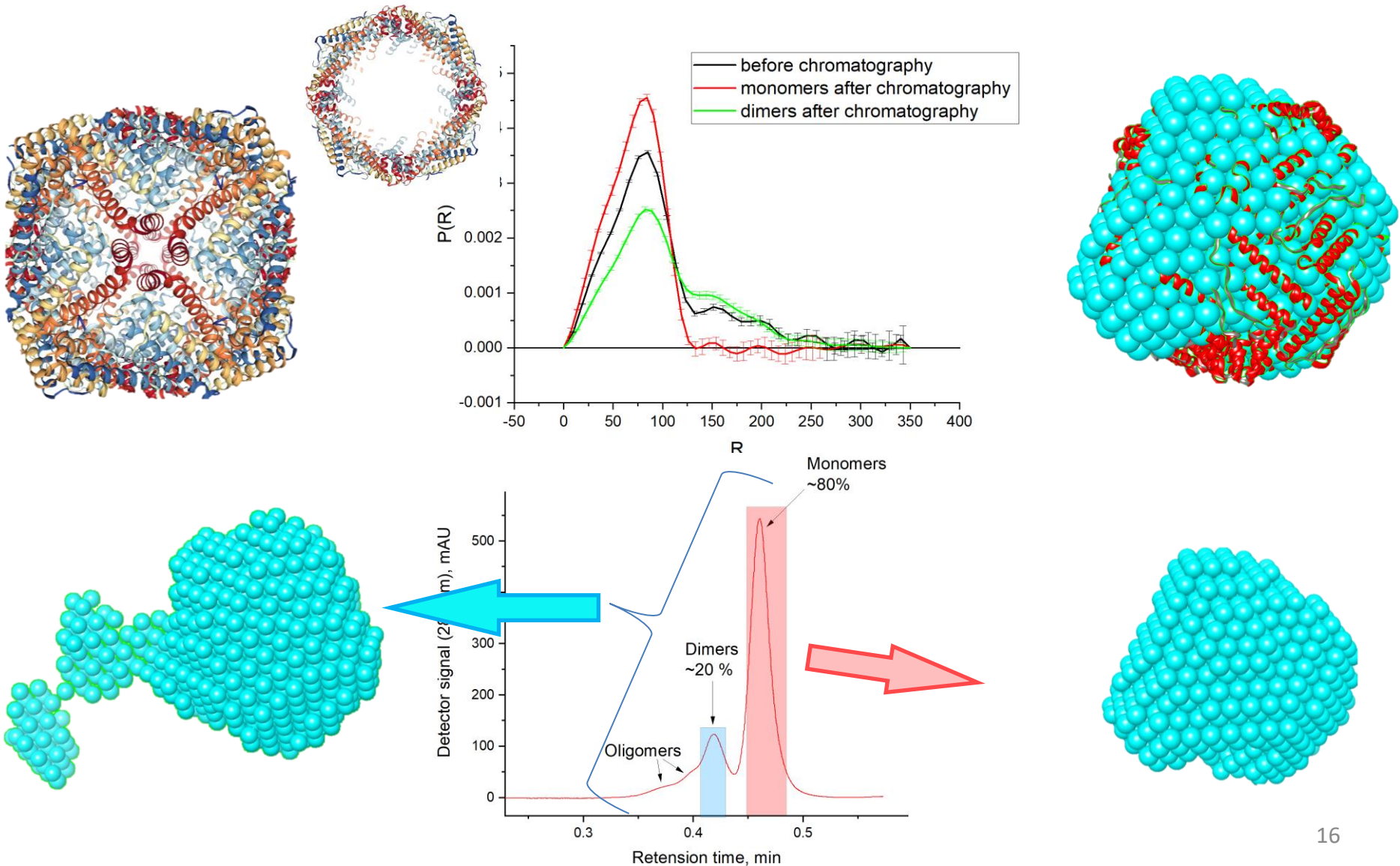
## Funding:

- RSF Grant (Kucerka N.)
- Department of Spectrometers Complex  
IBR-2 (Kulikov S., Bodnarchuk V.)
- JINR-Poland Grant (Kuklin A.)



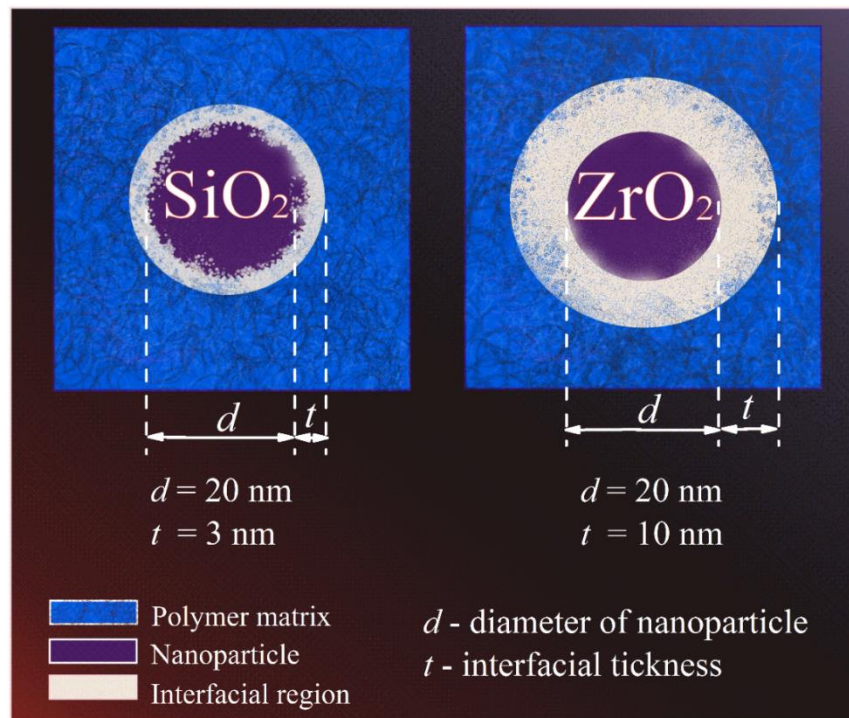
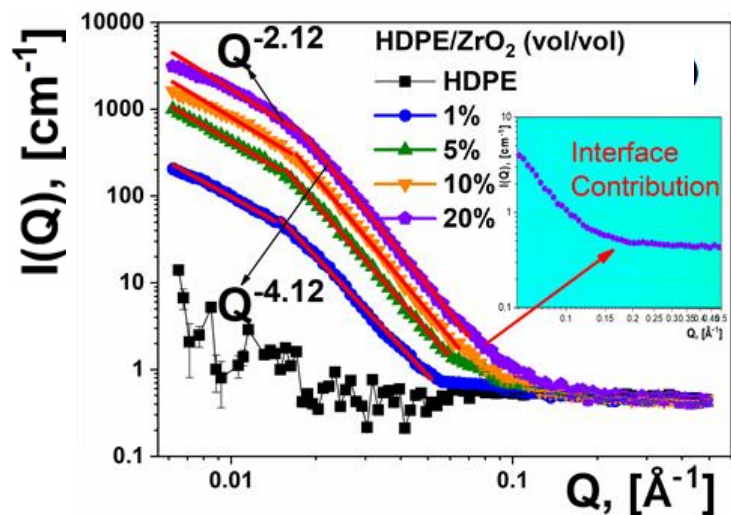
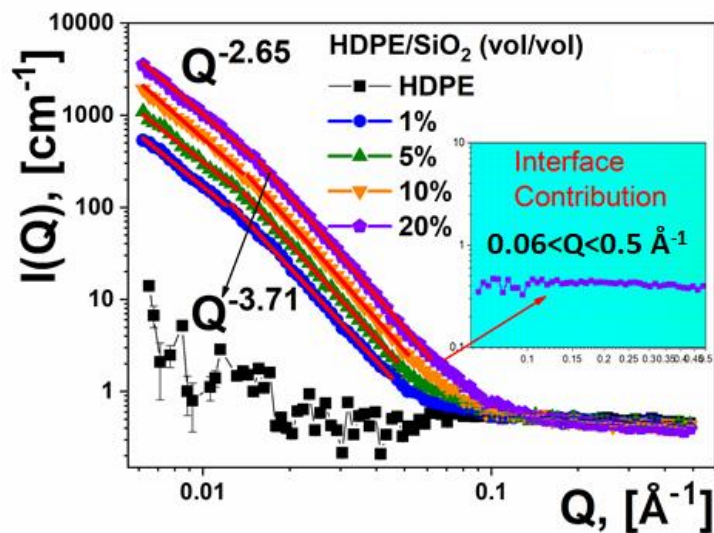
# Implementation of SEC on YuMO spectrometer

## Apoferritin protein





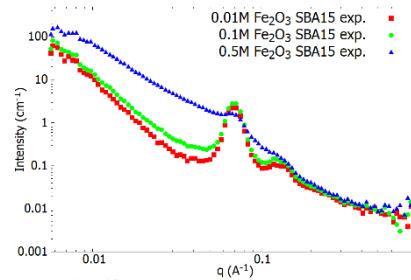
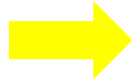
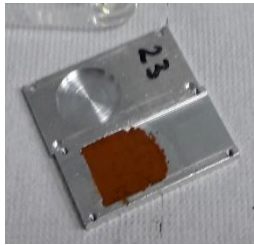
# Interfacial effects in polymer-nanoparticle composite films by small-angle neutron scattering method



Nabiyev, A.A.; Olejniczak, A.; Islamov, A.K.; Pawlukojs, A.; Ivankov, O.I.; Balasoiu, M.; et al. Composite Films of HDPE with SiO<sub>2</sub> and ZrO<sub>2</sub> Nanoparticles: The Structure and Interfacial Effects. *Nanomaterials* 2021, 11, 2673. <https://doi.org/10.3390/nano11102673>

# Nanopores for Magnetic and Biomedical Applications

## SANS experiments at YuMO



total SANS scattering = regular matrix + polydisperse spheres



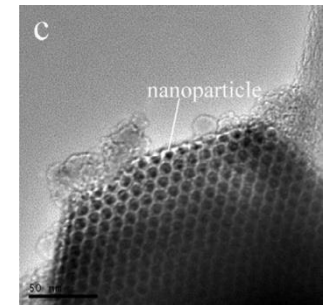
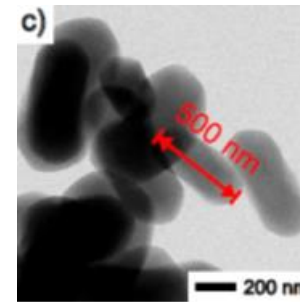
$$I(q) = K_C S(q) |F_C(q)|^2 + K_S |F_S(q)|^2 + I_d(q) + I_i$$

- pores - size & mutual distance
- NPs - size distribution & concentration

## Material

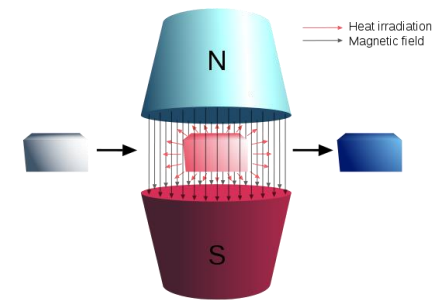
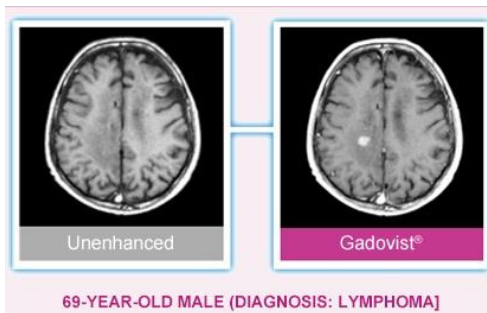
Periodic nanoporous silica

- perfect regular structure
- biocompatibility
- thermal stability and durability
- high specific surface



## Applications

- therapeutic agents in tumor treatment and drug delivery
- MRI contrast media (Gadovist)
- magnetic refrigeration due to the large magnetocaloric effect



# Size and distribution of the iron oxide nanoparticles in SBA-15 nanoporous silica via SANS study

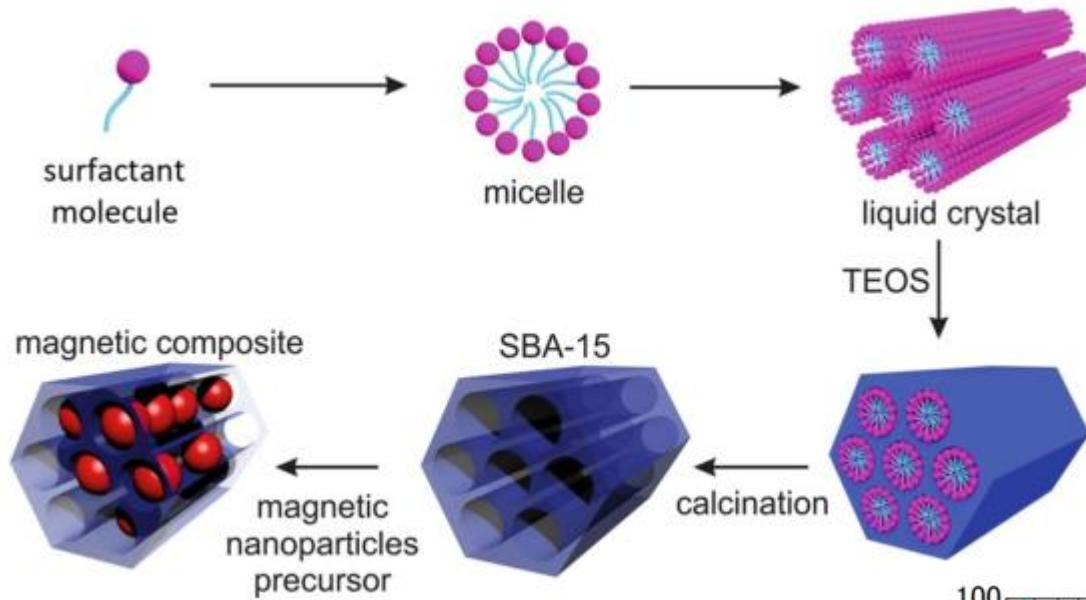
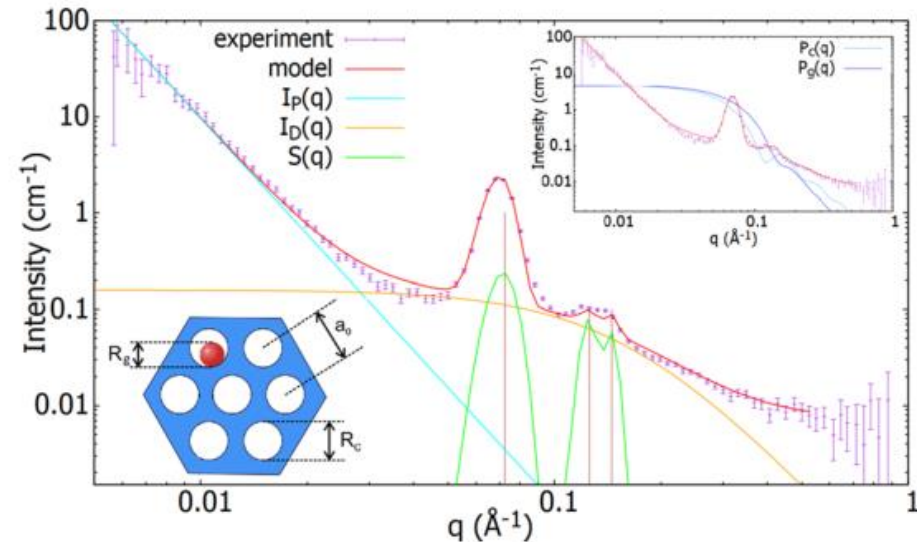
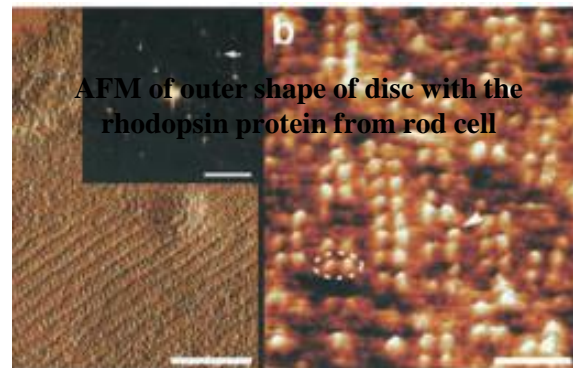
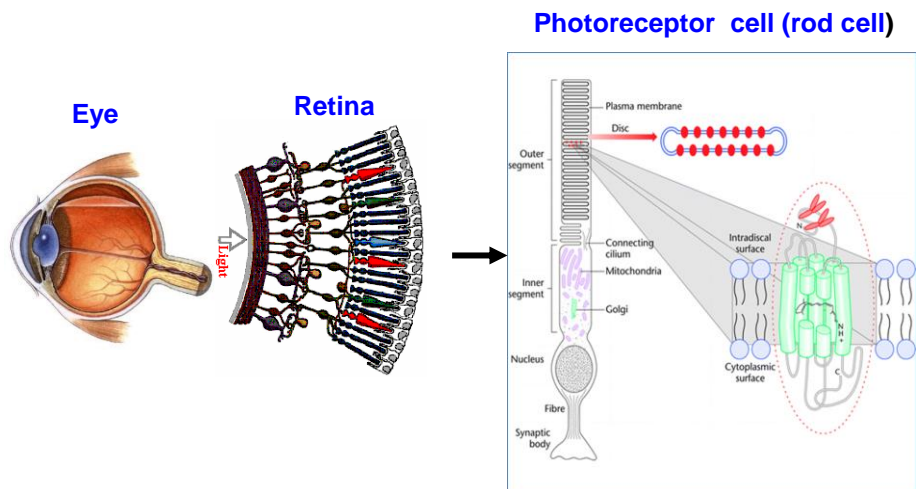


Illustration of the Fe<sub>2</sub>O<sub>3</sub>@SBA-15 nanocomposite preparation and structure organization. Polydisperse nanoparticles of Fe<sub>2</sub>O<sub>3</sub> are randomly distributed in the longitudinal cylindrical pores of perfect hexagonal order within silica matrix.

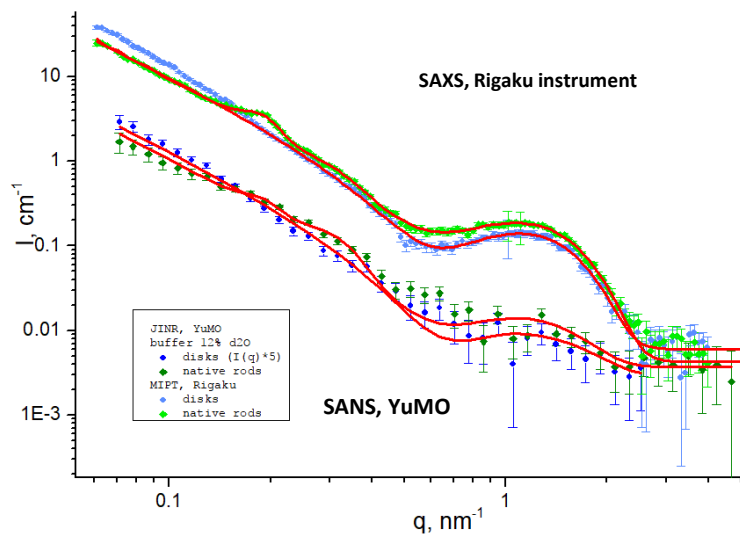
Fit of the model to the experimental SANS data corresponding to nanocomposite Fe<sub>2</sub>O<sub>3</sub>@SBA-15 (1) with very sparse occupation of the pores by nanoparticles



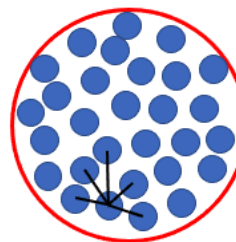
# Supramolecular organization of rhodopsin



Distance between rhodopsin centers 38 Å.  
Rhodopsin molecule size is 35 Å.



Photoreceptor membrane model (fragment)



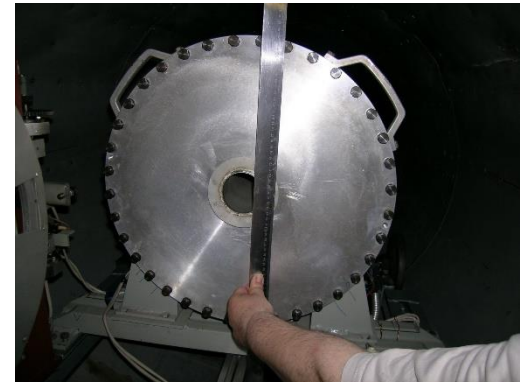
The average distance between the rhodopsin molecule centers is 58 Å

# Magnetic system



Main parameters:

- Magnetic field: up to 2 T.
- 
- 2 rotary planes
- 2 replaceable poles with the ability to change the distance between poles
- The gap is up to 130 mm.
- Weight about 2 tons.



**THANK YOU FOR YOUR ATTENTION!**

